Letter

Higher-order topological quantum paramagnets

Daniel González-Cuadra [*]

ICFO - Institut de Ciències Fotòniques, The Barcelona Institute of Science and Technology, Av. Carl Friedrich Gauss 3,
08860 Castelldefels (Barcelona), Spain;
Center for Quantum Physics, University of Innsbruck, 6020 Innsbruck, Austria;
and Institute for Quantum Optics and Quantum Information of the Austrian Academy of Sciences, 6020 Innsbruck, Austria

Quantum paramagnets are strongly correlated phases of matter where competing interactions frustrate magnetic order down to zero temperature. In certain cases, quantum fluctuations instead induce topological order, supporting fractionalized quasiparticles. In this Letter, we investigate paradigmatic spin models and show how magnetic frustration can also give rise to higher-order topological properties. We first study the frustrated Heisenberg model in a square lattice, where a plaquette valence bond solid appears through the spontaneous breaking of translational invariance. Despite the amount of effort that has been devoted to study this phase, its topological nature has so far been overlooked. By means of tensor network simulations, we establish how such a state belongs to a higher-order symmetry-protected topological phase, where long-range plaquette order and nontrivial topology coexist. Through this interplay, we uncover excitations that would be absent otherwise, such as cornerlike bulk states bound to dynamical topological defects. Finally, we demonstrate how this higher-order topological quantum paramagnet is also induced by dipolar interactions, indicating the possibility to directly observe this phase using atomic quantum simulators.

I. INTRODUCTION

Topology has emerged in the last decades as a central concept in theoretical physics, acting as a driving force in the search for novel phases of matter [1]. The growing interest in topological quantum states experienced in the last years has been fueled, in particular, by the outstanding experimental progress in ultracold atomic experiments [2–5], where such states can be prepared and investigated with an unprecedented degree of control [6–11], as well as by their applications in fault-tolerant quantum computation [12–14].

Although nontrivial topology exists in the absence of any symmetry [15], both notions are usually intertwined. For instance, symmetry-protected topological phases, recently realized in atomic platforms [16,17], are only robust to symmetry-preserving perturbations. In the last years, there has been growing interest in topological crystalline insulators [18], which are not protected by global [19] but rather pointlike symmetries [20]. Within this class, the recently discovered higher-order topological insulators (HOTIs) [21,22] present unusual properties that generalize the standard bulk-boundary correspondence [23]: they support gapless states in boundaries of codimensions larger that one, such as corner or hinge states [24,25]. Although noninteracting HOTIs have been extensively investigated and even realized experimentally [26–34], interacting higher-order symmetry-protected topological (HOSPT) phases are only starting to be explored [35–46].

In this Letter, we present an interaction-induced HOSPT phase driven by magnetic frustration: a higher-order topological quantum paramagnet (HOTQP). Quantum paramagnets (QPs) arise in spin models where competing interactions enhance quantum fluctuations, preventing magnetic order [47]. Of particular interest are spin liquids [48,49], which do not break any symmetry and can present topological order. The former usually compete with other QPs such as valence-bond solids (VBSs) that spontaneously break certain spatial symmetries. Here we show how the plaquette VBS (PVBS) in the frustrated Heisenberg model belongs to a HOSPT phase, representing an example of a quantum phase possessing both long-range order (LRO) due to spontaneous symmetry breaking (SSB) and nontrivial higher-order topology. We show how the interplay between these two features gives rise to strongly correlated topological effects. In particular, away from the zero-magnetization sector, dynamical topological defects appear in the plaquette order, hosting localized cornerlike states in the bulk.

The Letter is organized as follows. We first consider the Heisenberg model in a square lattice with interactions beyond nearest neighbors (NNs) and study a phase transition between a magnetically ordered and a PVBS phase. We then show how the latter belongs to a HOTQP phase by revealing its entanglement structure, as well as through a many-body topological invariant. These quantities are also used to characterize the topological phase transition between the trivial and the HOTQP phases, and to investigate the mechanism behind the emergence of topological defects. Finally, we study the Heisenberg model with dipolar interactions and show that its ground state is also a HOTQP. The dipolar Heisenberg model has gained attention in recent years [50–53], since it naturally

*daniel.gonzalez-cuadra@uibk.ac.at

appears as an effective description of ultracold molecules in optical lattices [54,55] and can also be simulated using trapped ions [56–59] and Rydberg atoms [60,61]. Ultracold molecules are particularly interesting for quantum simulation purposes due to their strong dipole interactions, and different schemes have been proposed to use them to simulate quantum magnetism [62–65] as well as topological phases [66–69]. Recent experimental progress has demonstrated how to cool, trap [70–74], and control interactions between molecules [75–77], indicating how the observation of a HOTQP could be within reach using near-term devices.

II. THE FRUSTRATED HEISENBERG MODEL

We start by considering the antiferromagnetic Heisenberg model on a two-dimensional square lattice,

$$\hat{H} = \sum_{i,j} J_{i,j} \hat{\mathbf{S}}_i \cdot \hat{\mathbf{S}}_j, \tag{1}$$

with $J_{i,j} > 0$. Here $\hat{\mathbf{S}}_i = (S_i^x, S_i^y, S_i^z)$ and $S_i^\mu = \frac{1}{2}\sigma_i^\mu$ are spin-1/2 operators and σ_i^μ are Pauli matrices. If only NN interactions are present, the SU(2) symmetry is spontaneously broken and the ground state develops magnetic LRO [78]. The latter is characterized by the spin structure factor,

$$S_L(\mathbf{q}) = \frac{1}{L^2} \sum_{i,j} \langle \hat{\mathbf{S}}_i \cdot \hat{\mathbf{S}}_j \rangle e^{i\mathbf{q}\cdot(\mathbf{r}_i - \mathbf{r}_j)}, \tag{2}$$

where $L \equiv L_x = L_y$ is the size of the lattice in each direction. In the zero-magnetization sector, $M = \sum_i \langle \hat{S}_i^z \rangle = 0$, with magnetization axis z, the ground state corresponds to a Néel state. This is signaled by a nonzero value of the Néel order parameter $S_\infty^N \equiv S_L(\mathbf{q} = (\pi, \pi))$ in the thermodynamic limit, $S_\infty^N \equiv \lim_{L\to\infty} S_L^N \neq 0$. Although the SU(2) symmetry is broken, the ground state is still invariant under U(1) rotations around the magnetization axis.

Longer-range interactions beyond NNs promote other types of magnetic LRO. Here we consider the $J_1 - J_2 - J_3$ Heisenberg model with interactions up to third-NNs, $J_{i,j} = J_1\delta_{|i-j|,1} + J_2\delta_{|i-j|,\sqrt{2}} + J_3\delta_{|i-j|,2}$. For $J_3 = 0$, the ground state is a collinear state at $\mathbf{q} = (0, \pi)$ or $\mathbf{q} = (\pi, 0)$ for $J_2/J_1 \gtrsim 0.6$ [79]. At intermediate values around the classical transition point, $J_2/J_1 = 0.5$, quantum fluctuations melt the magnetic order in a finite region, giving rise to a QP with $\lim_{L\to\infty} S_L(\mathbf{q}) = 0 \ \forall\mathbf{q}$. Although the nature of the resulting phase is disputed, density matrix renormalization group (DMRG) results point toward a PVBS phase [79,80]. This phase breaks translational invariance, giving rise to a plaquette structure in the NN correlators $\langle \hat{\mathbf{S}}_i \cdot \hat{\mathbf{S}}_j \rangle$, as shown in Fig. 1(a). The plaquette nonmagnetic LRO can be detected using the structure factor

$$S_L^P = \frac{1}{L^2} \sum_{\langle k,l \rangle} \epsilon(k, l)[\langle \hat{\mathbf{S}}_i \cdot \hat{\mathbf{S}}_j \hat{\mathbf{S}}_k \cdot \hat{\mathbf{S}}_l \rangle - \langle \hat{\mathbf{S}}_i \cdot \hat{\mathbf{S}}_j \rangle \langle \hat{\mathbf{S}}_k \cdot \hat{\mathbf{S}}_l \rangle], \tag{3}$$

where the sum runs over NN pairs $\langle k, l \rangle$. The pair $\langle i, j \rangle$ is fixed in the middle of the lattice and the form factor $\epsilon(k, l)$ is defined as in Ref. [81]. The PVBS phase is thus characterized by $S_\infty^P \equiv \lim_{L\to\infty} S_L^P \neq 0$.

For $J_3 \neq 0$, the PVBS phase appears around the frustration line $(J_2 + J_3)/J_1 = 0.5$ [81], where the classical energies of
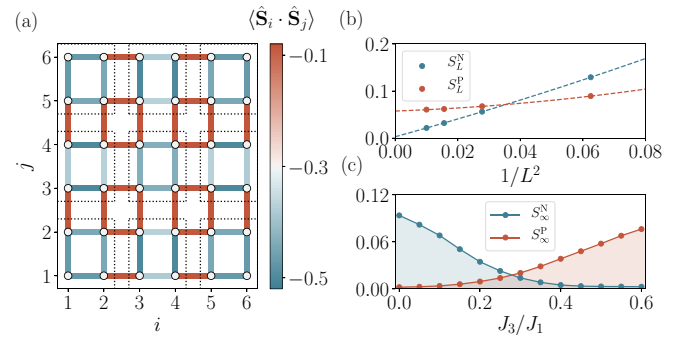

FIG. 1. Plaquette valence bond solid: (a) Real-space bond pattern $\langle \vec{S}_i \cdot \vec{S}_j \rangle$ for a lattice with $L^2 = 36$. For $J_3/J_1 = 0.6$ and $J_2 = 0$, the ground state belongs to a PVBS phase, characterized by a dimerized bond pattern both in the x and y directions and a four-site unit cell (marked by dotted squares in the figure). (b) Finite-size scaling for the Néel (S_L^N) and PVBS (S_L^P) order parameters for $J_3/J_1 = 0.5$. While the former vanishes in the thermodynamic limit, indicating a QP, the latter attains a finite value, associated with plaquette LRO. (c) Thermodynamic limit extrapolation $S_\infty^{N/P}$ as a function of J_3/J_1, indicating two distinct ordered phases.

the magnetically ordered states become equal. In the following, we fix $J_2 = 0$, where the value of S_∞^P is larger [81] and finite-size effects are reduced. We use a DMRG algorithm [82] with bond dimension $D = 1000$ to calculate the ground state of the model for various lattice sizes. In Fig. 1(b), we show how the finite-size scaling of S_L^P and S_L^N for $J_3/J_1 = 0.5$ is consistent with a PVBS phase. In Fig. 1(c), we show the thermodynamic limit extrapolation of the two order parameters, S_∞^N and S_∞^P, as a function of J_3/J_1. Although higher values of L^2 are required to obtain the precise transition point, our results, consistent with previous works [81,83,84], indicate the presence of two distinct phases, a Néel and a plaquette-ordered phase.

III. HIGHER-ORDER TOPOLOGICAL QUANTUM PARAMAGNETS

Although considerable effort has been devoted to the study of the PVBS, its topological properties have so far been overlooked. Here we claim that this state belongs to a HOSPT phase, which we call a HOTQP. The latter is protected by a U(1) × C_4 symmetry: conservation of the total magnetization M and rotational invariance. To see this, we first notice how the bond pattern spontaneously generated in the PVBS state resembles the pattern required to create one of the earliest examples of a HOSPT phase [36]. The latter corresponds to the ground state of a NN Heisenberg model, where J_1 varies in space according to a plaquettelike structure, similar to Fig. 1(a). In our case, however, such pattern arises in the bond correlators due to magnetic frustration via a SSB process starting from a translational invariant model.

To analyze the topological properties of the PVBS, we first focus on the structure of its entanglement spectrum (ES) [85]. We define a bipartition of the system and write the ground state as $|\psi_{gs}\rangle = \sum_n e^{-\epsilon_n/2}|\psi_n\rangle_A \otimes |\psi_n\rangle_B$, where A and B are two subsystems, and $\{\epsilon_n\}$ is the ES, that is, the eigenenergies of the entanglement Hamiltonian $\hat{H}_E$, defined through the
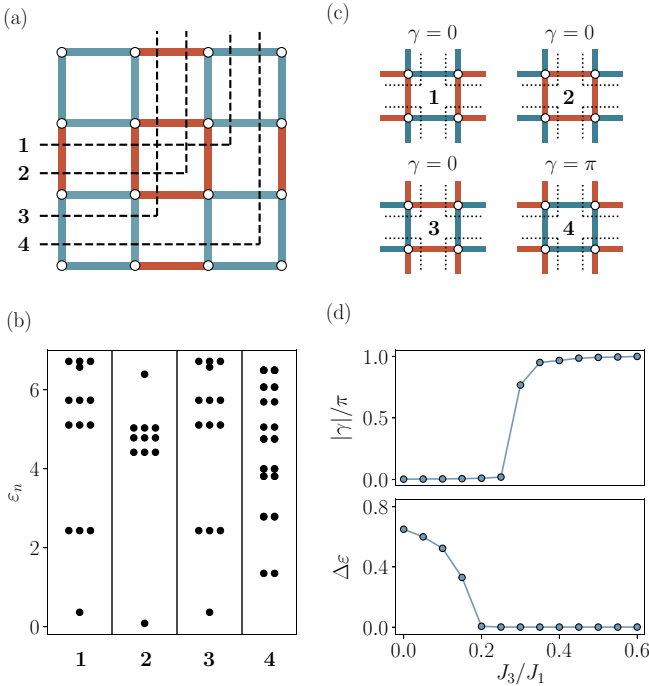
FIG. 2. Higher-order symmetry-protected topology: (a) In the figure, the dashed lines represent the four bipartitions used to study the ES. (b) Lower part of the ES for $L^2 = 16$ and $J_3/J_1 = 0.6$ and for each bipartition (c) Berry phase γ calculated at four different plaquettes in the middle of a lattice with $L^2 = 100$ and for $J_3/J_1 = 0.6$. A nontrivial phase of π is obtained at the same plaquette where the ES shows degeneracy when cut through. (d) γ and ES degeneracy $\Delta\epsilon$ as a function of J_3/J_1 for a $L^2 = 100$ lattice. The former is calculated at the central plaquette, while the latter is obtained through a bipartition between one corner and the rest of the system.

reduced density matrix $\rho_A = \mathrm{Tr}_B(|\Psi_{gs}\rangle\langle\Psi_{gs}|) = e^{-\hat{H}_E}$. The ES is degenerate for 1D topological phases [86], where cutting the chain into two halves creates a virtual edge, and this degeneracy is connected to the presence of localized states in the boundaries. For 2D HOSPT phases, the same occurs when a virtual corner is created, as shown in Fig. 2(a), associated in this case to the presence of corner states [87–89].

In Fig. 2(b), we show the lower part of the ES for different bipartitions of a system with $L^2 = 16$ in the PVBS phase [90]. The differences in the spectra stem from the inter- or intraunit cell nature of the cut. It is important to note that the PVBS has four degenerate ground states in the thermodynamic limit as a consequence of the SSB, only distinguished by the definition of the unit cell. Four different bipartitions in one of them thus provides the same information as cutting between unit cells for each ground state. Our results in Fig. 2(b) prove that one of them (No. 4 in the figure) is topologically nontrivial and is therefore expected to support localized corner states [21,91]. Due to finite-size effects, the lowest-energy state corresponds to configuration 2 in Fig. 2 [see also Fig. 1(a)], and thus lacks corner states [92]. We stress, however, that the HOSPT nature of the phase is encoded in each state, which, as we will see, will lead to nontrivial topological phenomena.

To support our claim, we compute a local Berry phase γ at different plaquettes for a system with $L^2 = 100$ [93]. The
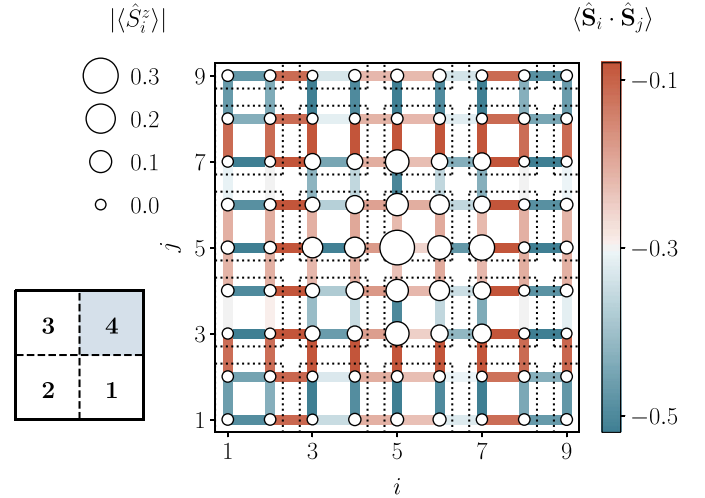
latter is a topological invariant that is quantized in the presence of the U(1) $\times C_4$ symmetry to values 0 and π for trivial and HOSPT states, respectively [94], serving as a many-body generalization of the quadrupole moment [21]. The results shown in Fig. 2(c) for the different values of γ coincide with those obtained for the ES, where we get $\gamma = \pi$ for the same plaquette that leads to degeneracy, and $\gamma = 0$ for the rest. Finally, we show for different values of J_3/J_1 both γ and the ES degeneracy $\Delta\epsilon = \sum_n (-1)^n \epsilon_n$, which is zero when the spectrum is degenerate. Although these quantities cannot be used to locate the transition point due to finite-size effects, which also prevent perfect quantization of γ, their behavior is consistent with the presence of two distinct phases: a trivial magnetically ordered phase and a topological PVBS phase. Finally, we note that the HOTQP phase can be regarded as a higher-order version of the Majumdar-Ghosh phase [95,96] in the $J_1 - J_2$ Heseinberg chain, a VBS with a doubly degenerate ground state, where one of them is topological [97].

IV. TOPOLOGICAL DEFECTS AND CORNERLIKE STATES

The combination of LRO and higher-order topology in the HOTQP gives rise to unique topological properties. To see this, we study the ground state for nonzero magnetization, taking a lattice with $L^2 = 81$ and $M = 1/2$. Figure 3 shows the real-space bond pattern for the ground state in the HOTQP phase, where two topological defects are created in the plaquette structure, as compared to the homogeneous $M = 0$ case [Fig. 1(a)]. The defects correspond to two 1D solitons that divide the system into four quadrants. Once the unit cell is defined, it becomes clear how each quadrant corresponds to each degenerate configuration of $M = 0$ [Fig. 29c]. Since

FIG. 3. Topological defects and cornerlike states: Real-space bond pattern $\langle\hat{\mathbf{S}}_i \cdot \hat{\mathbf{S}}_j\rangle$ for a lattice with $L^2 = 81$ and $M = 1/2$. Two one-dimensional solitons are formed in the plaquette-ordered pattern, one vertical and one horizontal, crossing at the center of the lattice. The two defects divide the system into four parts that correspond to the four degenerate ground states for $M = 0$, as indicated by the change in the unit cells (dotted squares) across the defects. One of them is topologically nontrivial and the defects act as a corner in the bulk, separating it from trivial regions. We present the net magnetization $|\langle\hat{S}_i^z\rangle|$, which reveals a localized spin at this bulk corner.

one of them is topologically nontrivial, the point where the two defects cross corresponds to a corner between the latter and a trivial bulk. A localized spin is expected precisely at this point and this is confirmed by the local magnetization $\langle |\hat{S}_i^z| \rangle$ (Fig. 3). We note that, although topological defects have been recently considered for HOTIs, in particular, disclinations [91,98–101] and dislocations [102,103], they correspond to static defects imposed externally. Our results show how localized cornerlike states emerge in the bulk from a translationally invariant model. These excitations are higher-order 2D versions of the localized states induced by solitons in the Su-Schrieffer-Heeger model [104], recently generalized to the bosonic case [105–108], and the Majumdar-Ghosh phase [97].

V. QUANTUM SIMULATION WITH ULTRACOLD MOLECULES

Although the frustrated Heisenberg model describes a variety of materials, observing a HOTQP can be challenging in solid-state devices. We now discuss the possibility of preparing this phase using quantum simulators based on ultracold molecules. Consider a 2D array of polar molecules in an optical lattice with frozen motional degrees of freedom, described as quantum rotors interacting via dipolar interactions [62–65]. One can choose two rotational states $|J, M\rangle$ to build spin operators, where J and M are the total and third components of the angular momentum operator $\hat{\mathbf{J}}$. For a strong enough external electric field aligned perpendicular to the lattice plane, and by taking $|\uparrow\rangle = |1, 0\rangle$ and $|\downarrow\rangle = |0, 0\rangle$), the system is described by the effective Hamiltonian [52],

$$\hat{H}_{\text{eff}} = \sum_{i,j} \frac{g}{|i-j|^3} \left[2d_{00}^2 \left(\hat{S}_i^x \hat{S}_j^x + \hat{S}_i^y \hat{S}_j^y \right) + (\mu_0 - d_0)^2 \hat{S}_i^z \hat{S}_j^z \right],$$
(4)

with $g = 1/(4\pi\epsilon_0)$, $d_{00} = \langle \uparrow |\hat{d}_z| \downarrow \rangle$, $d_0 = \langle \downarrow |\hat{d}_z| \downarrow \rangle$, and $\mu_0 = \langle \uparrow |\hat{d}_z| \uparrow \rangle$, where $\hat{d}_z$ is the third component of the dipole operator $\hat{\mathbf{d}}$. The Heisenberg point can be reached at $2d_{00}^2 = (\mu_0 - d_0)^2$ [52] by tuning the electric field, corresponding to Hamiltonian Eq. (1) with $J_{i,j} = 2g d_{00}^2/|i-j|^3$. The largest interaction terms are related by $(J_2 + J_3)/J_1 = 1/2^{3/2} + 1/2^3 \approx 0.479$, which is close to the frustration point 0.5. It is therefore natural to ask whether the ground state of the dipolar Heisenberg model in a square lattice is a HOTQP.

Previous works have studied the model using various approximations, founding a Néel ground state [50,51]. Using DMRG, which allows us to capture more correlations, we show that the Néel order parameter actually vanishes. Figure 4(a) shows the finite-size scaling of S_L^N for different truncations of the dipolar interactions, that is, keeping only the K largest terms. The results are consistent with a QP and for $K > 5$ the values do not change noticeably. Moreover, the scaling of S_L^P is consistent with a PVBS for every value of K [Fig. 4(b)]. Finally, we calculated the Berry phase and obtained a value of $\gamma = 0.97\pi$ for the same plaquette as in Fig. 2(c).

Our results therefore indicate that a HOTQP could be prepared using ultracold molecules in an optical lattice. The real-space plaquette structure, as well as the presence of topological defects and cornerlike states, could be revealed using a quantum gas microscope with single-site resolution
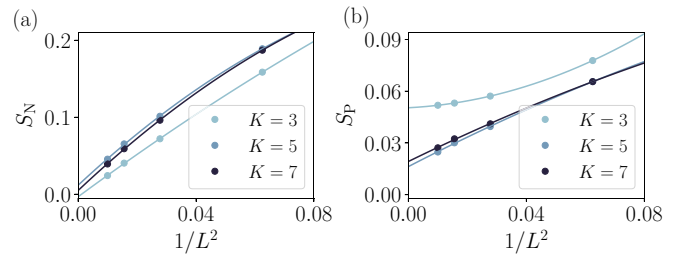

FIG. 4. Dipolar Heisenberg model: Finite-size scaling of the order parameters S_L^N and S_L^P in the ground state of the dipolar Heisenberg model for different truncations K of the dipolar interactions (see main text). The results are consistent with a PVBS.

[109–111]. The nontrivial topological properties could be accessed by measuring the ES, which can be efficiently achieved using near-term quantum simulators [112,113]. Here we focus on ultracold molecules, but similar physics could be simulated using trapped ions [56–59], magnetic [114], or Rydberg atoms [115], where spin models with dipolar interactions have already been realized [60,61,116,117].

VI. CONCLUSIONS AND OUTLOOK

In this Letter, we investigated how magnetic frustration can induce nontrivial higher-order topological properties. In particular, we studied the well-known PVBS in the frustrated Heisenberg model and we showed that it belongs to a HOTQP phase. Although we focus on the $J_1 - J_3$ model, our results could be generalized to any PVBS, in particular, to the ground state of the $J_1 - J_2$ model, since they are adiabatically connected. Moreover, we revealed how the interplay between LRO and higher-order topology gives rise to topological excitations, such as cornerlike states in the bulk bound to dynamical topological defects.

Our results show that spin liquids are not the only QPs with interesting topological properties and that a HOSPT phase was hiding in plain sight in paradigmatic spin models. Moreover, we show how this phase is stabilized by dipolar interactions, indicating how the corresponding physics could be further explored in quantum simulators, offering higher control compared to natural materials. Experiments with ultracold molecules or Rydberg atoms could achieve larger sizes than those accessible with classical simulations, facilitating, for instance, the study of the topological phase transition that gives rise to the HOTQP, as well as possible hidden topological properties in other VBS states. Finally, the role of vortex defects in the deconditioned nature [80,118] of the Néel to PVBS phase transition was recently studied [119]. It would thus be interesting to analyze the role of the solitons considered here to further elucidate the nature of the corresponding topological critical point, as well as to find other mechanisms that give rise to HOSPT phases induced by SSB.

[1] J. E. Moore, Nature (London) **464**, 194 (2010).

[2] D. Jaksch and P. Zoller, Ann. Phys. **315**, 52 (2005), Special Issue.

[3] M. Lewenstein, A. Sanpera, V. Ahufinger, B. Damski, A. Sen(De), and U. Sen, Adv. Phys. **56**, 243 (2007).

[4] C. Gross and I. Bloch, Science **357**, 995 (2017).

[5] F. Schäfer, T. Fukuhara, S. Sugawa, Y. Takasu, and Y. Takahashi, Nat. Rev. Phys. **2**, 411 (2020).

[6] M. Atala, M. Aidelsburger, J. T. Barreiro, D. Abanin, T. Kitagawa, E. Demler, and I. Bloch, Nat. Phys. **9**, 795 (2013).

[7] H. Miyake, G. A. Siviloglou, C. J. Kennedy, W. C. Burton, and W. Ketterle, Phys. Rev. Lett. **111**, 185302 (2013).

[8] M. Aidelsburger, M. Atala, M. Lohse, J. T. Barreiro, B. Paredes, and I. Bloch, Phys. Rev. Lett. **111**, 185301 (2013).

[9] G. Jotzu, M. Messer, R. Desbuquois, M. Lebrat, T. Uehlinger, D. Greif, and T. Esslinger, Nature (London) **515**, 237 (2014).

[10] M. Aidelsburger, M. Lohse, C. Schweizer, M. Atala, J. T. Barreiro, S. Nascimbène, N. R. Cooper, I. Bloch, and N. Goldman, Nat. Phys. **11**, 162 (2015).

[11] N. Goldman, J. C. Budich, and P. Zoller, Nat. Phys. **12**, 639 (2016).

[12] A. Kitaev, Ann. Phys. **303**, 2 (2003).

[13] H.-N. Dai, B. Yang, A. Reingruber, H. Sun, X.-F. Xu, Y.-A. Chen, Z.-S. Yuan, and J.-W. Pan, Nat. Phys. **13**, 1195 (2017).

[14] G. Semeghini, H. Levine, A. Keesling, S. Ebadi, T. T. Wang, D. Bluvstein, R. Verresen, H. Pichler, M. Kalinowski, R. Samajdar, A. Omran, S. Sachdev, A. Vishwanath, M. Greiner, V. Vuletic, and M. D. Lukin, arXiv:2104.04119.

[15] X.-G. Wen, Rev. Mod. Phys. **89**, 041004 (2017).

[16] S. de Léséleuc, V. Lienhard, P. Scholl, D. Barredo, S. Weber, N. Lang, H. P. Büchler, T. Lahaye, and A. Browaeys, Science **365**, 775 (2019).

[17] P. Sompet, S. Hirthe, D. Bourgund, T. Chalopin, J. Bibo, J. Koepsell, P. Bojović, R. Verresen, F. Pollmann, G. Salomon, C. Gross, T. A. Hilker, and I. Bloch, arXiv:2103.10421.

[18] L. Fu, Phys. Rev. Lett. **106**, 106802 (2011).

[19] C.-K. Chiu, J. C. Y. Teo, A. P. Schnyder, and S. Ryu, Rev. Mod. Phys. **88**, 035005 (2016).

[20] T. L. Hughes, E. Prodan, and B. A. Bernevig, Phys. Rev. B **83**, 245132 (2011).

[21] W. A. Benalcazar, B. A. Bernevig, and T. L. Hughes, Science **357**, 61 (2017).

[22] W. A. Benalcazar, B. A. Bernevig, and T. L. Hughes, Phys. Rev. B **96**, 245115 (2017).

[23] S. Ryu and Y. Hatsugai, Phys. Rev. Lett. **89**, 077002 (2002).

[24] F. Schindler, A. M. Cook, M. G. Vergniory, Z. Wang, S. S. P. Parkin, B. A. Bernevig, and T. Neupert, Sci. Adv. **4**, eaat0346 (2018).

[25] E. Khalaf, Phys. Rev. B **97**, 205136 (2018).

[26] S. Imhof, C. Berger, F. Bayer, J. Brehm, L. W. Molenkamp, T. Kiessling, F. Schindler, C. H. Lee, M. Greiter, T. Neupert, and R. Thomale, Nat. Phys. **14**, 925 (2018).

[27] C. W. Peterson, W. A. Benalcazar, T. L. Hughes, and G. Bahl, Nature (London) **555**, 346 (2018).

[28] M. Serra-Garcia, V. Peri, R. Süsstrunk, O. R. Bilal, T. Larsen, L. G. Villanueva, and S. D. Huber, Nature (London) **555**, 342 (2018).

[29] X. Ni, M. Weiner, A. Alù, and A. B. Khanikaev, Nat. Mater. **18**, 113 (2019).

[30] H. Xue, Y. Yang, F. Gao, Y. Chong, and B. Zhang, Nat. Mater. **18**, 108 (2019).

[31] H. Xue, Y. Yang, G. Liu, F. Gao, Y. Chong, and B. Zhang, Phys. Rev. Lett. **122**, 244301 (2019).

[32] S. N. Kempkes, M. R. Slot, J. J. van den Broeke, P. Capiod, W. A. Benalcazar, D. Vanmaekelbergh, D. Bercioux, I. Swart, and C. Morais Smith, Nat. Mater. **18**, 1292 (2019).

[33] M. Weiner, X. Ni, M. Li, A. Alù, and A. B. Khanikaev, Sci. Adv. **6**, eaay4166 (2020).

[34] M. S. Kirsch, Y. Zhang, M. Kremer, L. J. Maczewsky, S. K. Ivanov, Y. V. Kartashov, L. Torner, D. Bauer, A. Szameit, and M. Heinrich, Nat. Phys. **17**, 995 (2021).

[35] Y. You, T. Devakul, F. J. Burnell, and T. Neupert, Phys. Rev. B **98**, 235102 (2018).

[36] O. Dubinkin and T. L. Hughes, Phys. Rev. B **99**, 235132 (2019).

[37] K. Kudo, T. Yoshida, and Y. Hatsugai, Phys. Rev. Lett. **123**, 196402 (2019).

[38] K. Laubscher, D. Loss, and J. Klinovaja, Phys. Rev. Research **1**, 032017(R) (2019).

[39] K. Laubscher, D. Loss, and J. Klinovaja, Phys. Rev. Research **2**, 013330 (2020).

[40] A. Sil and A. K. Ghosh, J. Phys.: Condens. Matter **32**, 205601 (2020).

[41] A. Rasmussen and Y.-M. Lu, Phys. Rev. B **101**, 085137 (2020).

[42] J. Bibo, I. Lovas, Y. You, F. Grusdt, and F. Pollmann, Phys. Rev. B **102**, 041126(R) (2020).

[43] C. Peng, L. Zhang, and Z.-Y. Lu, Phys. Rev. B **104**, 075112 (2021).

[44] J. Guo, J. Sun, X. Zhu, C.-A. Li, H. Guo, and S. Feng, J. Phys.: Condens. Matter **34** 035603 (2021).

[45] A. Hackenbroich, A. Hudomal, N. Schuch, B. A. Bernevig, and N. Regnault, Phys. Rev. B **103**, L161110 (2021).

[46] Y. Otsuka, T. Yoshida, K. Kudo, S. Yunoki, and Y. Hatsugai, Sci. Rep. **11**, 20270 (2021).

[47] C. Lacroix, P. Mendels, and F. Mila, *Introduction to Frustrated Magnetism: Materials, Experiments, Theory*, Vol. 164 (Springer Science & Business Media, Berlin Heidelberg, 2011), Vol. 164.

[48] L. Savary and L. Balents, Rep. Prog. Phys. **80**, 016502 (2016).

[49] Y. Zhou, K. Kanoda, and T.-K. Ng, Rev. Mod. Phys. **89**, 025003 (2017).

[50] H. Zou, E. Zhao, and W. V. Liu, Phys. Rev. Lett. **119**, 050401 (2017).

[51] A. Keleş and E. Zhao, Phys. Rev. B **97**, 245105 (2018).

[52] N. Y. Yao, M. P. Zaletel, D. M. Stamper-Kurn, and A. Vishwanath, Nat. Phys. **14**, 405 (2018).

[53] A. Keleş and E. Zhao, Phys. Rev. Lett. **120**, 187202 (2018).

[54] M. A. Baranov, M. Dalmonte, G. Pupillo, and P. Zoller, Chem. Rev. **112**, 5012 (2012).

[55] J. L. Bohn, A. M. Rey, and J. Ye, Science **357**, 1002 (2017).

[56] D. Porras and J. I. Cirac, Phys. Rev. Lett. **92**, 207901 (2004).

[57] T. Graß and M. Lewenstein, EPJ Quantum Technol. **1**, 8 (2014).

[58] A. Bermudez, L. Tagliacozzo, G. Sierra, and P. Richerme, Phys. Rev. B **95**, 024431 (2017).

[59] C. Monroe, W. C. Campbell, L.-M. Duan, Z.-X. Gong, A. V. Gorshkov, P. W. Hess, R. Islam, K. Kim, N. M. Linke, G. Pagano, P. Richerme, C. Senko, and N. Y. Yao, Rev. Mod. Phys. **93**, 025001 (2021).

[60] S. Geier, N. Thaicharoen, C. Hainaut, T. Franz, A. Salzinger, A. Tebben, D. Grimshandl, G. Zürn, and M. Weidemüller, Science **374**, 1149 (2021).

[61] P. Scholl, H. J. Williams, G. Bornet, F. Wallner, D. Barredo, T. Lahaye, A. Browaeys, L. Henriet, A. Signoles, C. Hainaut, T. Franz, S. Geier, A. Tebben, A. Salzinger, G. Zürn, and M. Weidemüller, arXiv:2107.14459.

[62] A. Micheli, G. K. Brennen, and P. Zoller, Nat. Phys. **2**, 341 (2006).

[63] R. Barnett, D. Petrov, M. Lukin, and E. Demler, Phys. Rev. Lett. **96**, 190401 (2006).

[64] A. V. Gorshkov, S. R. Manmana, G. Chen, J. Ye, E. Demler, M. D. Lukin, and A. M. Rey, Phys. Rev. Lett. **107**, 115301 (2011).

[65] A. V. Gorshkov, S. R. Manmana, G. Chen, E. Demler, M. D. Lukin, and A. M. Rey, Phys. Rev. A **84**, 033619 (2011).

[66] N. Y. Yao, A. V. Gorshkov, C. R. Laumann, A. M. Läuchli, J. Ye, and M. D. Lukin, Phys. Rev. Lett. **110**, 185302 (2013).

[67] S. R. Manmana, E. M. Stoudenmire, K. R. A. Hazzard, A. M. Rey, and A. V. Gorshkov, Phys. Rev. B **87**, 081106(R) (2013).

[68] A. V. Gorshkov, K. R. Hazzard, and A. M. Rey, Mol. Phys. **111**, 1908 (2013).

[69] D. Peter, N. Y. Yao, N. Lang, S. D. Huber, M. D. Lukin, and H. P. Büchler, Phys. Rev. A **91**, 053617 (2015).

[70] K.-K. Ni, S. Ospelkaus, M. H. G. de Miranda, A. Pe'er, B. Neyenhuis, J. J. Zirbel, S. Kotochigova, P. S. Julienne, D. S. Jin, and J. Ye, Science **322**, 231 (2008).

[71] J. Deiglmayr, A. Grochola, M. Repp, K. Mörtlbauer, C. Glück, J. Lange, O. Dulieu, R. Wester, and M. Weidemüller, Phys. Rev. Lett. **101**, 133004 (2008).

[72] K.-K. Ni, S. Ospelkaus, D. Wang, G. Quéméner, B. Neyenhuis, M. H. G. de Miranda, J. L. Bohn, J. Ye, and D. S. Jin, Nature (London) **464**, 1324 (2010).

[73] J. W. Park, S. A. Will, and M. W. Zwierlein, Phys. Rev. Lett. **114**, 205302 (2015).

[74] L. De Marco, G. Valtolina, K. Matsuda, W. G. Tobias, J. P. Covey, and J. Ye, Science **363**, 853 (2019).

[75] A. Chotia, B. Neyenhuis, S. A. Moses, B. Yan, J. P. Covey, M. Foss-Feig, A. M. Rey, D. S. Jin, and J. Ye, Phys. Rev. Lett. **108**, 080405 (2012).

[76] B. Yan, S. A. Moses, B. Gadway, J. P. Covey, K. R. A. Hazzard, A. M. Rey, D. S. Jin, and J. Ye, Nature (London) **501**, 521 (2013).

[77] K. R. A. Hazzard, B. Gadway, M. Foss-Feig, B. Yan, S. A. Moses, J. P. Covey, N. Y. Yao, M. D. Lukin, J. Ye, D. S. Jin, and A. M. Rey, Phys. Rev. Lett. **113**, 195302 (2014).

[78] E. Fradkin, *Field Theories of Condensed Matter Physics*, 2nd ed. (Cambridge University Press, Cambridge, 2013).

[79] S.-S. Gong, W. Zhu, D. N. Sheng, O. I. Motrunich, and M. P. A. Fisher, Phys. Rev. Lett. **113**, 027201 (2014).

[80] L. Wang, Z.-C. Gu, F. Verstraete, and X.-G. Wen, Phys. Rev. B **94**, 075143 (2016).

[81] M. Mambrini, A. Läuchli, D. Poilblanc, and F. Mila, Phys. Rev. B **74**, 144422 (2006).

[82] J. Hauschild and F. Pollmann, Sci. Post Phys. Lect. Notes, 5 (2018).

[83] V. Murg, F. Verstraete, and J. I. Cirac, Phys. Rev. B **79**, 195119 (2009).

[84] J. Reuther, P. Wölfle, R. Darradi, W. Brenig, M. Arlego, and J. Richter, Phys. Rev. B **83**, 064416 (2011).

[85] H. Li and F. D. M. Haldane, Phys. Rev. Lett. **101**, 010504 (2008).

[86] F. Pollmann, A. M. Turner, E. Berg, and M. Oshikawa, Phys. Rev. B **81**, 064439 (2010).

[87] T. Fukui and Y. Hatsugai, Phys. Rev. B **98**, 035147 (2018).

[88] Y. You, J. Bibo, and F. Pollmann, Phys. Rev. Research **2**, 033192 (2020).

[89] O. Dubinkin and T. L. Hughes, arXiv:2002.08385.

[90] The ES was calculated here by first computing the corresponding reduced density matrix associated. For most bipartitions, such calculation is computationally intractable for large system sizes. Nevertheless, our results show that, despite possible finite-size effects, the ES is degenerate even in the case of a small lattice with $L^2 = 16$.

[91] W. A. Benalcazar, T. Li, and T. L. Hughes, Phys. Rev. B **99**, 245151 (2019).

[92] The ground-state configuration that supports corner states can be obtained numerically by adding a small perturbation that breaks the degeneracy and promotes it energetically. This, however, requires larger systems than those that could be accessed here with enough accuracy, where the energy difference between these states is smaller and so would be the required perturbation.

[93] The local Berry phase is calculated by locally deforming the Hamiltonian with complex phases around a plaquette and calculating the corresponding Berry phase through a Wilson loop. For further technical details, we refer to Ref. [94].

[94] H. Araki, T. Mizoguchi, and Y. Hatsugai, Phys. Rev. Research **2**, 012009(R) (2020).

[95] C. K. Majumdar and D. K. Ghosh, J. Math. Phys. **10**, 1388 (1969).

[96] C. K. Majumdar and D. K. Ghosh, J. Math. Phys. **10**, 1399 (1969).

[97] S. Birnkammer, A. Bohrdt, F. Grusdt, and M. Knap, arXiv:2012.09185.

[98] S. Liu, A. Vishwanath, and E. Khalaf, Phys. Rev. X **9**, 031003 (2019).

[99] T. Li, P. Zhu, W. A. Benalcazar, and T. L. Hughes, Phys. Rev. B **101**, 115115 (2020).

[100] Y. Liu, S. Leung, F.-F. Li, Z.-K. Lin, X. Tao, Y. Poo, and J.-H. Jiang, Nature (London) **589**, 381 (2021).

[101] C. W. Peterson, T. Li, W. Jiang, T. L. Hughes, and G. Bahl, Nature (London) **589**, 376 (2021).

[102] R. Queiroz, I. C. Fulga, N. Avraham, H. Beidenkopf, and J. Cano, Phys. Rev. Lett. **123**, 266802 (2019).

[103] B. Roy and V. Juricic, Phys. Rev. Research **3**, 033107 (2021).

[104] W. P. Su, J. R. Schrieffer, and A. J. Heeger, Phys. Rev. Lett. **42**, 1698 (1979).

[105] D. González-Cuadra, A. Dauphin, P. R. Grzybowski, P. Wójcik, M. Lewenstein, and A. Bermudez, Phys. Rev. B **99**, 045139 (2019).

[106] D. González-Cuadra, A. Bermudez, P. R. Grzybowski, M. Lewenstein, and A. Dauphin, Nat. Commun. **10**, 2694 (2019).

[107] D. González-Cuadra, A. Dauphin, P. R. Grzybowski, M. Lewenstein, and A. Bermudez, Phys. Rev. Lett. **125**, 265301 (2020).

[108] D. González-Cuadra, A. Dauphin, P. R. Grzybowski, M. Lewenstein, and A. Bermudez, Phys. Rev. B **102**, 245137 (2020).

[109] W. S. Bakr, J. I. Gillen, A. Peng, S. Fölling, and M. Greiner, Nature (London) **462**, 74 (2009).

[110] J. F. Sherson, C. Weitenberg, M. Endres, M. Cheneau, I. Bloch, and S. Kuhr, Nature (London) **467**, 68 (2010).

[111] J. P. Covey, L. D. Marco, Ó. L. Acevedo, A. M. Rey, and J. Ye, New J. Phys. **20**, 043031 (2018).

[112] C. Kokail, R. van Bijnen, A. Elben, B. Vermersch, and P. Zoller, Nat. Phys. **17**, 936 (2021).

[113] C. Kokail, B. Sundar, T. V. Zache, A. Elben, B. Vermersch, M. Dalmonte, R. van Bijnen, and P. Zoller, Phys. Rev. Lett. **127**, 170501 (2021).

[114] T. Lahaye, C. Menotti, L. Santos, M. Lewenstein, and T. Pfau, Rep. Prog. Phys. **72**, 126401 (2009).

[115] A. Browaeys and T. Lahaye, Nat. Phys. **16**, 132 (2020).

[116] A. de Paz, A. Sharma, A. Chotia, E. Maréchal, J. H. Huckans, P. Pedri, L. Santos, O. Gorceix, L. Vernac, and B. Laburthe-Tolra, Phys. Rev. Lett. **111**, 185305 (2013).

[117] A. de Paz, P. Pedri, A. Sharma, M. Efremov, B. Naylor, O. Gorceix, E. Maréchal, L. Vernac, and B. Laburthe-Tolra, Phys. Rev. A **93**, 021603(R) (2016).

[118] T. Senthil, A. Vishwanath, L. Balents, S. Sachdev, and M. P. A. Fisher, Science **303**, 1490 (2004).

[119] Y. You, Z. Bi, and M. Pretko, Phys. Rev. Research **2**, 013162 (2020).